



Research article

The spatiotemporal epidemiological study on human brucellosis in shenyang, China from 2013 to 2022

Huijie Chen^{a,b}, Lihai Wen^a, Ye Chen^a, Xingyu Ji^a, Peng Li^{a,b,*}, Wei Sun^{b,**}

^a Department of Infectious Disease, Shenyang Municipal Center for Disease Control and Prevention, Shenyang, Liaoning, PR China

^b Key Laboratory of Early Warning and Intervention Technologies and Countermeasures for Major Public Health Events in Liaoning Province, China Medical University, Shenyang, Liaoning, PR China

ARTICLE INFO

Keywords:

Human brucellosis
Spatiotemporal epidemiological characteristics
Shenyang

ABSTRACT

Background: Epidemiological characteristics of human brucellosis (HB) have changed over the last decade. In this study, we depicted the spatiotemporal features of HB in Shenyang, China, from 2013 to 2022 and the objective was to visualise spatiotemporal patterns and identify high-risk regions with the purpose to provide evidence for HB prevention and control.

Methods: We performed an observational epidemiological study using HB data obtained from the National Notifiable Disease Reporting System (NNDRS). Joinpoint regression analysis was employed to determine the changing trends in the annual incidence. A vector boundary map of Shenyang was used to visualise spatial distribution. Spatial autocorrelation was identified using both global and local Moran's autocorrelation coefficients, while hotspot areas were determined using the Getis-Ord statistic.

Results: A combined sum of 4103 HB cases were analysed, and the average level of annual incidence of HB was 5.52 per 100,000. The incidence of HB showed obvious seasonality, with a notable peak observed from April to July (summer peak). The annual incidence in Shenyang has been on the rise since 2013, with an annual percentage change (APC) of 6.39% (95%CI 1.29%, 12.39%). Xinmin County exhibited the most elevated average annual incidence rate, with Faku County ranking second. The average annual incidence in rural areas exhibited a significantly greater disparity compared to suburban areas ($P < 0.001$), whereas the incidence rate in suburban areas demonstrated a significantly higher contrast when compared to urban areas ($P < 0.001$). A clustered distribution of the annual incidence of HB was observed for all years from 2013 to 2022. Abnormally high values were found in suburban areas, and no abnormally high values were found after 2017. The low-low clustering areas were found in urban as well as suburban areas from 2013 to 2022. Hotspots ($P < 0.05$) were located in rural areas, while cold spots ($P < 0.05$) were found in both urban and suburban areas. Since 2020, there have been no hotspots in Shenyang.

Conclusions: Rural areas are high-risk areas for HB and may be key to controlling HB epidemics. Although the annual incidence of HB in rural areas has increased, owing to the stability of spatial relationships and the disappearance of hotspots, there is little possibility of outbreaks; however, stricter monitoring should be applied in rural areas to prevent the emergence of new transmission routes.

* Corresponding author. Department of Infectious Disease, Shenyang Municipal Center for Disease Control and Prevention, No.88 Langming Street, Shenyang, 110163, PR China.

** Corresponding author. Key Laboratory of Early Warning and Intervention Technologies and Countermeasures for Major Public Health Events in Liaoning Province, China Medical University, No.77 Puhe Road, Shenyang, 110122, PR China.

E-mail addresses: sylclp@163.com (P. Li), wsun@cmu.edu.cn (W. Sun).

<https://doi.org/10.1016/j.heliyon.2024.e29026>

Received 10 July 2023; Received in revised form 27 March 2024; Accepted 28 March 2024

Available online 3 April 2024

2405-8440/© 2024 The Authors. Published by Elsevier Ltd. This is an open access article under the CC BY-NC license (<http://creativecommons.org/licenses/by-nc/4.0/>).

1. Introduction

Brucellosis, as a zoonotic disease, commonly transmits to humans via direct contact with animals that have contracted the infection, including sheep, cattle, goats, pigs, and dogs. The infection usually occurs when individuals consume unpasteurized milk products or come into contact with contaminated tissues like aborted placentas without proper protection [1,2]. Individuals who work with animals, in abattoirs or as veterinarians face an increased likelihood of acquiring the infection [3]. Human brucellosis (HB) typically presents as a gradual onset of pyrexia, fatigue, nocturnal diaphoresis (accompanied by a distinct and atypical musty odor), and arthralgias [4]. HB can affect any organ and complications are common [5,6]. These complications may manifest as infections in one or multiple focal sites, potentially leading to conditions such as osteoarticular disease, genitourinary issues, cardiovascular problems, pulmonary disorders, dermatologic indications, and adverse outcomes during pregnancy [6]. Most cases can be treated successfully with a standard regimen. However, relapse and therapeutic failure may occur when intracellular bacteria are not eradicated [7,8]. Although HB is rarely fatal, it generally debilitates individuals [6] and causes heavy social and economic burdens [4,6,9].

Annually, around half a million instances of HB are documented globally [10], with an estimated susceptible population of 2.4 billion individuals [11]. The rapid progress in socioeconomic status and growing public health concerns have had a great impact on HB incidence distribution, and the worldwide geographical pattern of HB shows that developed nations have a lower incidence, while underdeveloped nations have a higher incidence [12]. The prevalence of HB in Northern Europe, Canada, Australia, and New Zealand has been effectively controlled or eliminated with an incidence rate of less than 0.2 cases per 100,000 individuals [13,14]. In contrast, Central and Southwest Asian countries are currently experiencing a significant surge in cases [14]. Syria reports the highest incidence of HB at 40.6 per 100,000, followed by Iran at 18.6 per 100,000 [15].

In China, research has consistently indicated a rise in the occurrence of HB since the mid-1990s, reaching its peak in 2014 at a rate of 4.2 cases per 100,000 individuals [16,17]. However, the incidence of HB decreased from 2014 to 2018 and rebounded in 2019 [18,19]. Recent research in 2021 has shown that the incidence of HB may reach five cases per 100,000 people [20]. The rebound can be primarily attributed to the resurgence of this disease in the Inner Mongolia Autonomous Region and failure to achieve the control objectives outlined in the National Brucellosis Prevention and Control Plan (NBPCP), which was implemented between 2016 and 2020 with aims to contain both animal and human transmission across China [21,22]. Spatial autocorrelation analysis showed a non-random distribution in China, and high-high clusters were observed in northern China, where 95.5% of total cases were centralised, whereas low-low clusters were found in the southern regions [17,18,20]. Research has also shown that HB has extended from its traditional pastoral areas in the north to urban areas in the central region [19].

Liaoning Province is located in northeastern China. Research has shown that since 2001, there has been an annual increase in the incidence of HB [23–25]. Incidence rates from 2020 to 2021 showed that although Liaoning ranks 7th in China (6.8 cases per 100,000 individuals in 2020, 12.8 cases per 100,000 individuals in 2021), the increasing amplitude is the second highest in China, reaching 87.8% [20]. In Shenyang, the capital city of Liaoning Province, 15% of the population originates from rural areas where livestock farming is prevalent. Studies have shown that from 2009 to 2015, the incidence of HB in Shenyang increased annually, especially in Xinmin, which had the highest incidence [26]. Shenyang borders the Inner Mongolia Autonomous Region, which is renowned for its elevated prevalence rate in China and frequent livestock trading activities. These factors somewhat increase the risk of acquiring the disease. Currently, HB epidemics are an important public health concern, particularly in resource-limited regions. Therefore, it is necessary to investigate the HB epidemics in Shenyang.

In this study, we depicted the spatiotemporal characteristics of HB in Shenyang following the approach employed by Liang et al. [17]. The aim of this research was to visualise spatiotemporal patterns and identify high-risk regions with the purpose to provide evidence for HB prevention and control.

2. Methods

2.1. Study area

Shenyang, located in Liaoning province, China (latitude ranging from 41°11' to 43°02'N and longitude spanning from 122°25' to 123°48'E). The city is officially designated as a prefecture-level administrative division and covers an expansive area of 12,860 square kilometers. It encompasses a total of 13 districts [27], which follows the criteria of distinction between urban and rural areas that is widely used worldwide [28], Heping, Shenhe, Dadong, Huanggu, and Tiexi districts were defined as urban areas; Sujiatun, Hunnan, Shenbeixin, and Yuhong districts were defined as suburban areas; Liaozhong, Kangping, Faku, and Xinmin counties were defined as rural areas, according to their population density and economic development in this study. The average population of Shenyang was 7,431,458 from 2013 to 2022.

2.2. Data sources

An observational epidemiological study was employed for this study. All reported cases (including time of onset, diagnosis, and report, as well as the individual's age, gender, profession, and residential location) of HB in Shenyang, China from January 1, 2013 to December 31, 2022 were extracted from the Nationwide Notifiable Infectious Diseases Reporting Information System (NIDRIS) which was utilized under authorized permission and not publicly accessible. All eligible HB cases were identified based on clinical indicators and laboratory tests, while excluding individuals who did not reside in Shenyang, duplicate reports, and cases of recurrence.

Population data were retrieved from the Official Website of Shenyang Statistical Bureau (<http://tjj.shenyang.gov.cn/>). A vector boundary map of Shenyang was downloaded from the Data Sharing Infrastructure of Earth System Science (<http://www.geodata.cn/>).

2.3. Case definition

The classification of HB falls under Group B infectious diseases according to the Law on Prevention and Treatment of Infectious Diseases in the People’s Republic of China [29]. It is the result of infection by *Brucella* genus and must be reported through the NIDRIS within 24 h [30]. HB was diagnosed based on the Health Industry Standards for HB established by the National Health Commission of the People’s Republic of China [31], in which HB was confirmed when bacteria were detected through biochemical techniques or isolated from various sources such as blood, urine, cerebrospinal fluid, synovial fluid, pleural fluid, bone marrow, or liver biopsy. In this study, duplicate cases were defined as those in which two or more records existed in a single course of the disease, in which they had the same onset dates and the interval between them did not exceed one treatment cycle (6 weeks). Recurrent cases were defined as those that recurred after cure, in which they had different onset dates and the interval between them exceeded one treatment cycle (6 weeks). However, cases of recurrence have not been reported using the NIDRIS.

2.4. Spatial autocorrelation analysis

The annual incidence rate at the district level was utilized for the spatial autocorrelation analysis. The disease distribution including clustered, dispersed, or randomly distributed patterns was identified by global spatial autocorrelation (Global Moran’s *I*) statistic. If Moran’s *I* index values are close to +1.0, it represents that positive spatial autocorrelation occurs, which indicates the similar values cluster together. By contrast, if Moran’s *I* index values are close to −1.0, it represents that negative spatial autocorrelation occurs, which indicates the dissimilar values cluster together, in a term of dispersed pattern. If Moran’s *I* values are close to zero, it indicates no autocorrelation and is recognized as randomly distributed pattern [17,32]. The formal representation of the statistic can be written as

$$I = \frac{n}{\sum_{i=1}^n \sum_{j=1}^n W_{ij}} \frac{\sum_{i=1}^n \sum_{j=1}^n W_{ij}(y_i - \bar{y}) - (y_j - \bar{y})}{\sum_{i=1}^n (y_i - \bar{y})^2} \quad (i \neq j) \tag{1}$$

I represents the Moran’s *I* value, where *n* denotes the overall count of districts. The annual incidences of brucellosis in districts *i* and *j* are denoted by *y_i* and *y_j*, respectively. The average attribute value of all districts is represented as \bar{y} , while *w_{ij}* signifies the spatial weight between districts *i* and *j* [17,32].

Local spatial autocorrelation analysis (Anselin local Moran’s *I*) was applied to recognize the influential observations and outliers [33], in which, whether the value of an observation and the average of its surroundings were either more similar (high-high (HH) or low-low (LL)) or dissimilar (high-low (HL), low-high (LH)) than is expected from pure chance which was determined at a given probability level $P \leq 0.05$ using 999 randomisations. The local Moran’s *I* statistic can be written as [17,32]:

$$I = \frac{n^2(y_i - \bar{y}) \sum_{j=1}^n w_{ij}(y_j - \bar{y})}{\sum_{i=1}^n (y_i - \bar{y})^2} \tag{2}$$

Here, the symbols convey identical connotations as those found in the formal definition of Global Moran’s *I*

2.5. Hotspot analysis

The statistical measure for hotspot analysis (Getis-Ord, *G_i^{*}*) was employed to assess the strength and consistency of clusters in space, offering a benefit of identifying clusters with high-high value (hot spots) or low-low value (cold spots). If the *Z* (*G_i^{*}*) score is positive and statistically significant, it suggests that a particular district and its surrounding areas experience a relatively high occurrence of HB incidents, thus considering the area a hotspot. In contrast, if the *Z* (*G_i^{*}*) score is found to be both negative and statistically significant, it indicates that a particular district and its surrounding areas exhibit a comparatively lower occurrence of HB incidents, thereby being classified as a cold spot. In general, districts with *Z*-scores greater than 2.58 or *Z*-scores less than −2.58 were deemed statistically significant at a confidence level of 99% ($P < 0.01$). Districts with *Z*-scores ranging from 1.96 to 2.58 or from −2.58 to −1.96 were considered statistically significant at a confidence level of 95% ($P < 0.05$). Districts with *Z*-scores falling within the range of 1.65–1.96 or −1.96 to −1.65 were deemed statistically significant at a confidence level of 90% ($P < 0.10$) [34]. The Getis-Ord, *G_i^{*}* statistic can be written as

$$G_i^* = \frac{\sum_{j=1}^n W_{ij}y_j - \bar{y}\sum_{j=1}^n W_{ij}}{\sqrt{\frac{s}{n-1} \left[n \sum_{j=1}^n w_{ij}^2 - \left(\sum_{j=1}^n w_{ij} \right)^2 \right]}} \tag{3}$$

Table 1
Annual incidence of human brucellosis in different groups in Shenyang from 2013 to 2022.

Group	2013	2014	2015	2016	2017	2018	2019	2020	2021	2022	Average
	N(1/100,000)										
Total	264(3.64)	321(4.4)	341(4.67)	440(6.01)	369(5.02)	438(5.91)	392(5.22)	454(5.98)	711(9.31)	373(4.87)	410.3(5.52)
Gender											
Male	199(5.52)	243(6.72)	256(7.08)	336(9.28)	259(7.14)	319(8.74)	296(8.02)	315(8.45)	521(13.91)	261(6.96)	300.5(8.2)
Female	65(1.78)	78(2.12)	85(2.3)	104(2.81)	110(2.96)	119(3.17)	96(2.52)	139(3.6)	190(4.89)	112(2.87)	109.8(2.92)
χ^2	69.842	87.521	89.072	127.537	63.987	97.102	108.427	74.471	166.857	65.697	94.445
P	0.000	0.000	0.000	0.000	0.000	0.000	0.000	0.000	0.000	0.000	0.000
Age group(Years)											
0-9	6(1.19)	4(0.76)	12(2.22)	10(1.81)	3(0.53)	5(0.86)	7(1.16)	7(1.12)	12(1.91)	6(0.98)	7.2(1.25)
10-19	10(1.86)	10(1.96)	8(1.61)	10(2.05)	2(0.41)	6(1.21)	8(1.6)	8(1.57)	13(2.53)	7(1.33)	8.2(1.62)
20-29	31(3.18)	29(3.06)	29(3.16)	40(4.61)	28(3.49)	36(4.84)	23(3.27)	29(4.3)	24(3.67)	8(1.26)	27.7(3.5)
30-39	40(3.46)	43(3.71)	40(3.43)	60(5.03)	54(4.36)	72(5.65)	61(4.73)	49(3.76)	96(7.43)	43(3.47)	55.8(4.53)
40-49	56(4.16)	88(6.92)	92(7.56)	140(11.9)	105(9.05)	97(8.41)	86(7.46)	119(10.37)	170(14.83)	82(6.98)	103.5(8.66)
50-59	79(5.85)	95(6.8)	104(7.44)	113(8.18)	119(8.84)	128(9.65)	137(10.21)	141(10.39)	238(17.18)	138(9.9)	129.2(9.45)
60-69	30(3.91)	46(5.46)	49(5.3)	60(5.99)	51(4.74)	86(7.51)	58(4.88)	88(7.26)	131(10.82)	75(6.17)	67.4(6.37)
70-79	11(2.64)	6(1.44)	7(1.68)	7(1.67)	7(1.65)	8(1.84)	11(2.39)	12(2.41)	22(4.08)	14(2.4)	10.5(2.28)
80-90	1(0.49)	(0)	(0)	(0)	(0)	(0)	1(0.38)	1(0.38)	5(1.89)	(0)	0.8(0.33)
χ^2	94.445	84.427	89.425	140.048	147.319	120.809	131.457	163.769	253.664	162.517	121.946
P	0.000	0.000	0.000	0.000	0.000	0.000	0.000	0.000	0.000	0.000	0.000

Here, \bar{y} represents the average of attribute values across all districts, while s denotes the standard deviation, and the other symbols convey identical connotations as those found in the formal definition of Global Moran's I .

2.6. Statistical analysis

The annual incidence from 2013 to 2022 was calculated by dividing the number of new cases by the susceptible population and then multiplying it by 100,000 to obtain a whole number. The epidemiological attributes across temporal, spatial, and demographic aspects were analysed using Microsoft Excel 2019. The temporal trends were analysed using version 4.8.0.1 of the Joinpoint Regression Program, which calculated the annual percentage change (APC) along with corresponding 95% confidence intervals. A confidence interval of zero indicates no evidence to reject the null hypothesis (i.e., $APC = 0$), while positive or negative APC values indicate increasing or decreasing trends, respectively. Additionally, stationary trends were also identified. The criterion for determining statistical significance was set at a level of $P < 0.05$. The statistical analysis was conducted using SPSS software, specifically version 23.0. Measurements that followed a normal distribution were represented by the mean (\bar{x}) and standard deviation (s). A t -test was employed to compare the two groups, while analysis of variance (ANOVA) was utilized for group comparisons. Incidence rates were used to express count data, and the chi-square test was applied for intergroup comparisons. ArcGIS Desktop software (version 10.8; Esri Inc.; Redlands, California, USA) was used for global and local spatial autocorrelation, hot-spot analysis, visual presentation of the results, and mapping the spatial distribution of HB incidence in a vector boundary map of Shenyang at the district level for each year to highlight any spatial changes in risk over time.

3. Results

3.1. Demographic characteristics

A total of 7187 HB cases were reported from 2013–2022 with the exclusion of 3045 cases due to non-residency in Shenyang by the patients. In addition, 39 duplicate cases have been reported. Ultimately, the analysis included a total of 4103 cases. The average level of annual incidence of HB was 5.52 cases per 100,000 individuals. The average level of annual incidence among males (8.20 per 100,000) was found to be significantly greater than that observed in females (2.92 per 100,000) ($P < 0.001$). The annual average incidence exhibited a significant difference across different age groups ($P < 0.001$), with the highest incidence observed among individuals aged between 50 and 59 years (9.45 per 100,000). The distribution of the annual incidence in sex and age groups from 2013 to 2022 is shown in Table 1. Supplemental Fig. 1 shows that the main population affected by HB was farmers, followed by households, and unemployed personnel. Farmers accounted for approximately 64.85% of the total cases, ranging from 41.06% to 73.47% from 2013 to 2022, whereas household and unemployed personnel accounted for approximately 26.64% of the total cases, ranging from 20.66% to 45.48% from 2013 to 2022.

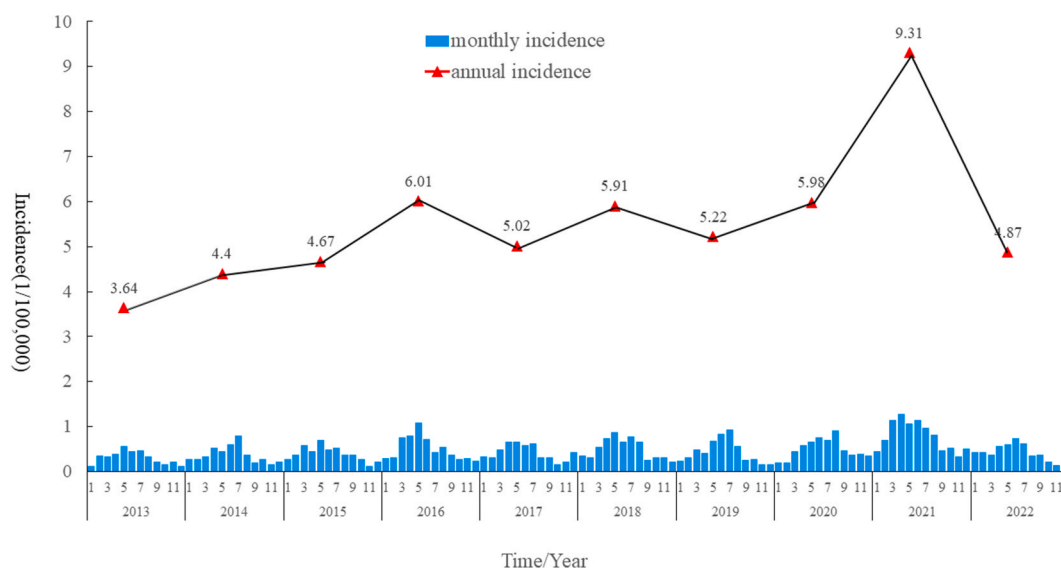


Fig. 1. Annual incidence and monthly incidence of human brucellosis in Shenyang, China from 2013–2022. The line chart shows the change trend of annual incidence of human brucellosis in Shenyang from 2013 to 2022. The bar chart shows the change trend of monthly incidence of human brucellosis from 2013 to 2022.

3.2. Temporal pattern

As shown in Fig. 1, the monthly incidence distribution of HB showed clear seasonality in Shenyang. The period from April to July (summer peak) exhibits a notable surge. From 2013 to 2021, the annual incidence of HB showed an upward trend. After reaching its peak in 2021, it dropped sharply in 2022. Supplemental Fig. 2 shows the findings from joinpoint regression analysis, which revealed that the annual incidence of HB in Shenyang has been on the rise since 2013, with an APC of 6.39% (1.29%, 12.39%). At the district/county level, there has been a consistent upward trend in the annual incidence of HB in both Xinmin and Liaozhong counties since 2013; the APC was 15.49% (6.61%, 29.51%) and 9.66% (2.32%, 18.89%), respectively. The annual incidence of HB in Yuhong has been decreasing since 2013, when the APC was -10.51% (-16.75% , -5.13%). There was no significant difference in the change in the annual incidence since 2013 in other districts/counties.

3.3. Spatial pattern

As shown in Supplemental Table 1 and Fig. 2, there was observed variation in the annual incidence of HB at the district/county scale in Shenyang between 2013 and 2022. It was found that Xinmin County exhibited the highest average annual incidence, closely followed by Faku County. Heping, Shenhe, Dadong, Huanggu, and Tiexi districts had the lowest average incidences. The annual average incidence in rural areas (314.4 per 100,000) demonstrated a significantly higher rate compared to suburban areas (64.8 per 100,000) ($P < 0.001$), while the annual average incidence in suburban areas was notably higher compared to that observed in urban areas (31.1 per 100,000) ($P < 0.001$).

3.4. Spatial autocorrelation analysis and hotspot analysis

The district/county level analysis of the annual incidence of HB in Shenyang revealed a spatially clustered distribution pattern, as indicated by the results of Global Moran's I (Table 2) for all years between 2013 and 2022. Fig. 3 displays the findings from Anselin local Moran's I analysis, which identified abnormally high values were all found in suburban areas. In 2013 and 2016, an abnormally high value was found in Shenbeixin district. In 2014, abnormally high values were found in Sujiatun and Yuhong district. In 2016, abnormally high values were found in Hunnan and Shenbeixin district. No abnormalities were found between 2017 and 2022. Low-low clustering areas were all found in urban and suburban areas. In 2013 and 2016, they were found in all urban areas and two suburban

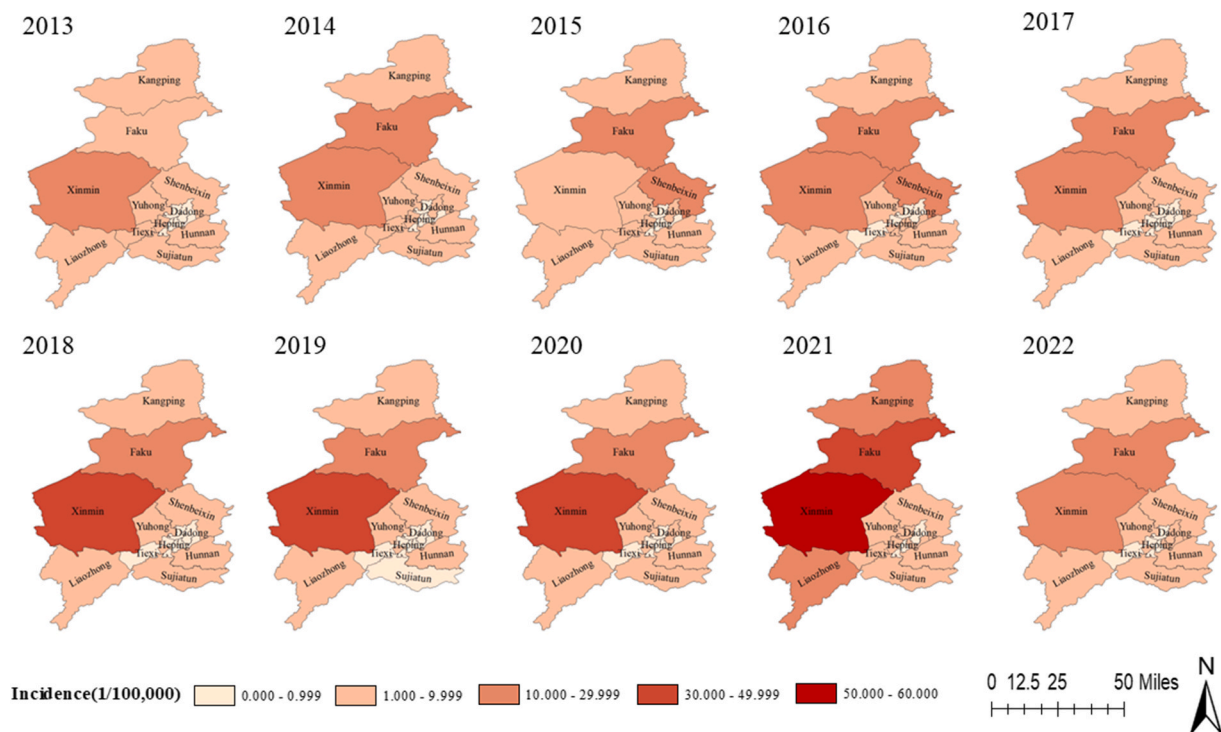


Fig. 2. The spatial distribution of human brucellosis in different districts/counties Shenyang, China from 2013–2022. The annual incidence of human brucellosis per 100,000 residents in each district/county in Shenyang from 2013 to 2022 are shown in the maps. The annual incidence of human brucellosis has a positive relationship with color darkness. The darker hues represent higher incidence rates, while the lighter shades indicate lower rates. These maps were produced by ArcGIS software version 10.8 (ESRI Lnc., Redlands, California, USA). (For interpretation of the references to color in this figure legend, the reader is referred to the Web version of this article.)

areas (Sujiatun and Hunnan district). In 2014, they were found in all urban areas and two suburban areas (Hunnan and Shenbeixin district). In 2015, they were found in all urban areas and one suburban area (Sujiatun district). From 2017 to 2022, they were found in all urban areas and three suburban areas (Sujiatun, Hunnan, and Shenbeixin district). The impact of the annual incidence in rural areas on the spatial autocorrelation of HB in Shenyang was not significant.

Hotspot analysis (Getis-Ord, G_i^*) of the annual incidence of HB at the district/county scale in Shenyang from 2013 to 2022 are shown in Fig. 4. From 2013 to 2019, all hotspots ($P < 0.05$) were located in rural areas. Xinmin county was a hotspot in 2013 and 2017–2019, Kangping and Faku county were hotspots in 2014–2016, and no hotspots were found in 2020–2022. No hotspots had been found in urban and suburban areas since 2013. Cold spots ($P < 0.05$) were found in both urban and suburban areas from 2013 to 2022, and all urban areas and two suburban areas (Sujiatun and Handong district) were cold spots from 2013 to 2022. Shenbeixin district was also a cold spot in 2014 and 2022, and no cold spots were found in rural areas since 2013.

4. Discussion

In this study, the average level of annual incidence of HB was observed to be 5.52 per 100,000 individuals in Shenyang, Liaoning Province, which was higher than that in China [16–20] and in Xian, Shanxi Province [35], but lower than that in Shanxi Province [36, 37], the Inner Mongolia Autonomous Region [38,39], and Liaoning Province [24,25]. Shenyang, the capital city of Liaoning Province and Xian, the capital city of Shanxi Province, exhibit a higher degree of urbanization compared to other cities in their respective provinces. This urbanization is accompanied by relatively less developed livestock husbandry. Consequently, it can be inferred that the lower incidence of HB in provincial capital cities as compared to the entire province may be attributed to these factors. In addition, in this study, we also found that the annual incidence rate peaked in 2021 since 2013, which aligned with the outcomes of prior studies [40,41]. Studies showed that the increase in both the population of sheep and individuals involved in animal husbandry brought out this momentum [20,41]. However, our finding may have a connection with that: i) the joint prevention and control mechanism of HB interrupted owing to the impact of the COVID-19, and the inadequate implementation of quarantine measures caused an increase of infectors [42]; ii) in 2020, people's travel had been restricted, as well as the insufficient laboratory test in hospitals because of the impact of COVID-19, leading to failing of detection. However, after the normalization management in 2021, the restriction of traffic lifted and the patients fully diagnosed, resulting in a sharp increase in the annual incidence [43].

In this study, we found that male farmers aged 40–59 years were the most affected by HB, which was consistent with previous research findings [23–25,36,44]. This may be related to the fact that this group was the main labour force in rural areas, and they earned their livelihood through the rearing of sheep, goats, and cattle. Studies have shown that the main endemic strain in Shenyang is the sheep strain [23–25]. It is common for farmers to engage in the handling of aborted placentas, shearing of wool, as well as the processing and trading of various meat products without utilizing personal protective gear like gloves, aprons, or masks [45,46], and these feeding methods increase the potential risk of infection by infected livestock where *Brucella* is reserved [47,48]. In addition, our study also found that households and unemployed personnel accounted for approximately 26.64% of the total cases, ranging from 20.66% to 45.48% from 2013 to 2022. These individuals were not engaged in livestock husbandry and did not participate in animal feeding but may have consumed unpasteurized milk products and unquarantined meat products [24]. This indicates that foodborne transmission is also an important route to acquire HB, and HB knowledge dissemination should continue to be strengthened to increase awareness of prevention and control so that residents do not buy unsterilised milk products and unquarantined meat products. Thus it can be seen that as a zoonotic disease, a potential threat to human's health located in livestock. However, human's life is closely connected with livestock and their products. In the past few years, some researchers have proposed the concept of One Health, which emphasized the close linkage and interdependence between the health of humans, animals, and the environment [49]. Therefore, the importance of One Health concept should also be fully recognized to tackle HB in the future.

The HB epidemic showed clear seasonal patterns, with its highest levels observed during the late spring and early summer periods [23–26,36,37,50]. Our study found that the monthly incidence distribution of HB had obvious seasonality in Shenyang, and a large peak occurred between April and July, which was consistent with previous findings. This period coincides with the lambing season (e. g. lamb delivery and breeding), potentially leading to increased chances of encountering *Brucella* [51].

Examining the spatial distribution of a disease proves advantageous in providing guidance for modifying and executing preventive

Table 2

Global spatial autocorrelation analysis (Global Moran's I) of the annual incidence of human brucellosis at districts/counties level in Shenyang, China, 2013–2022.

Year	Moran's I	Z Score	P Value	Aggregation
2013	0.226	3.623	0.001	YES
2014	0.292	4.585	0.000	YES
2015	0.135	2.579	0.009	YES
2016	0.166	2.943	0.003	YES
2017	0.176	2.935	0.003	YES
2018	0.169	2.881	0.004	YES
2019	0.160	2.722	0.006	YES
2020	0.171	2.869	0.004	YES
2021	0.201	3.253	0.001	YES
2022	0.261	4.051	0.000	YES

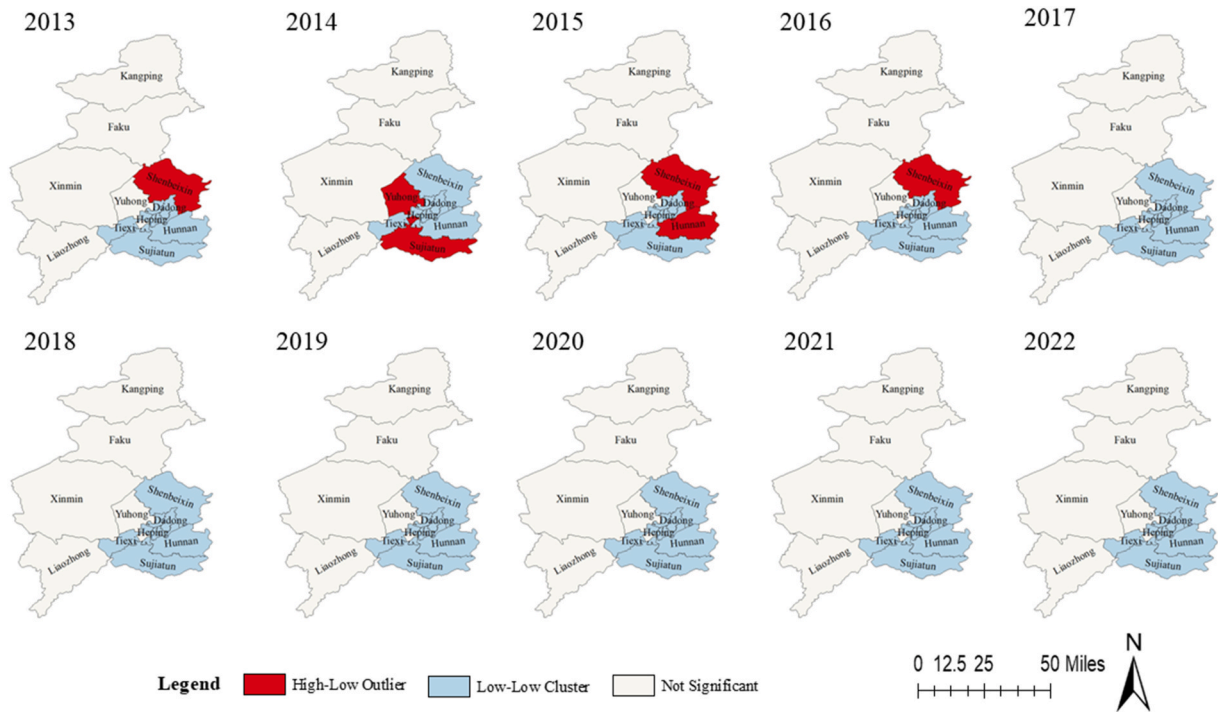


Fig. 3. Local spatial autocorrelation analysis (Anselin local Moran's I) of the annual incidence of human brucellosis at districts/counties level in Shenyang, China, 2013–2022. Bright red indicates a High-Low correlation, light red indicates a High-High correlation, light blue indicates a Low-Low correlation, and brown indicates no correlation. These maps were produced by ArcGIS software version 10.8 (ESRI Lnc., Redlands, California, USA). (For interpretation of the references to color in this figure legend, the reader is referred to the Web version of this article.)

and control strategies. In our study, disease mapping and time-pattern analysis were utilized to illustrate the spatial distribution and variation characteristics of HB incidence. Spatial distribution revealed a concentration of HB cases in rural areas with a lower economic development level and a more developed livestock industry. The incidence of HB was considerably elevated in rural areas as opposed to suburban and urban areas. Urban areas had the lowest annual incidence. This finding suggests that the incidence of HB is related to economic development. In addition, temporal pattern analysis showed an increasing trend since 2013 in Xinmin County and Liaozhong County; however, a downward trend was found in Yuhong district. As defined in this study, Xinmin and Liaozhong County belonged to rural areas and Yuhong District belonged to suburban areas, indicating that rural areas were the hardest hit areas of HB, and the situation was worsening; therefore, more attention should be paid to rural areas for the prevention and control of HB. As an intermediate area between urban and rural areas, the annual incidence of HB in partially suburban areas showed a moderating status, suggesting that there are fewer opportunities for residents living in suburban areas to contact infected animals and to increase personal hygiene awareness. However, this study also showed a relatively higher annual incidence in suburban areas, suggesting that effective measures for preventing and controlling HB in suburban areas, such as strict animal product quarantine and health education, should continue.

Spatial autocorrelation and hotspot analyses were employed to explore the spatial relationships of HB in different districts/counties. The analysis of global autocorrelation for the Global Moran's I value revealed a significant clustering pattern in the spatial distribution of HB in Shenyang from 2013 to 2022. This means that there existed a positive correlation between districts/counties, indicating high-high-value clustering or low-low-value clustering between adjacent districts/counties. The analysis of Local spatial autocorrelation (Anselin local Moran's I) showed abnormally high values and low-low clustering. Interestingly, i) the abnormally high values were all located in suburban areas, and no abnormally high values have been found since 2017; ii) the low-low clustering areas were all located in urban areas and partial suburban areas, and the spatial pattern has remained stable since 2017; iii) no kind of local clustering occurred in rural areas. These suggested that: i) the sudden increase of the incidence in suburban areas may be the key to the variation of spatial relationship; ii) some distinct influencing factors which were different from that in urban areas and rural areas may exist in suburban areas before 2017, but the effect of this influence declined after 2017, which may be related to the fact that, with the acceleration of urbanization, the lifestyle, health awareness and behaviour between residents in suburban areas and urban areas are becoming more similar; iii) the transmission routes of HB in rural areas were relatively fixed, such as the relatively fixed livestock feeding areas, the relatively fixed livestock feeding groups and patterns, as well as the relatively fixed livestock trading which was spontaneous between residents in Shenyang and the Inner Mongolia Autonomous Region, and had not yet emerged new routes strong enough to significantly increase the incidence of HB in the region. To maintain the stability of the spatial relationship of HB, it was crucial to prioritize the prevention of rebound incidents in suburban regions and implement more stricter monitoring in rural areas to

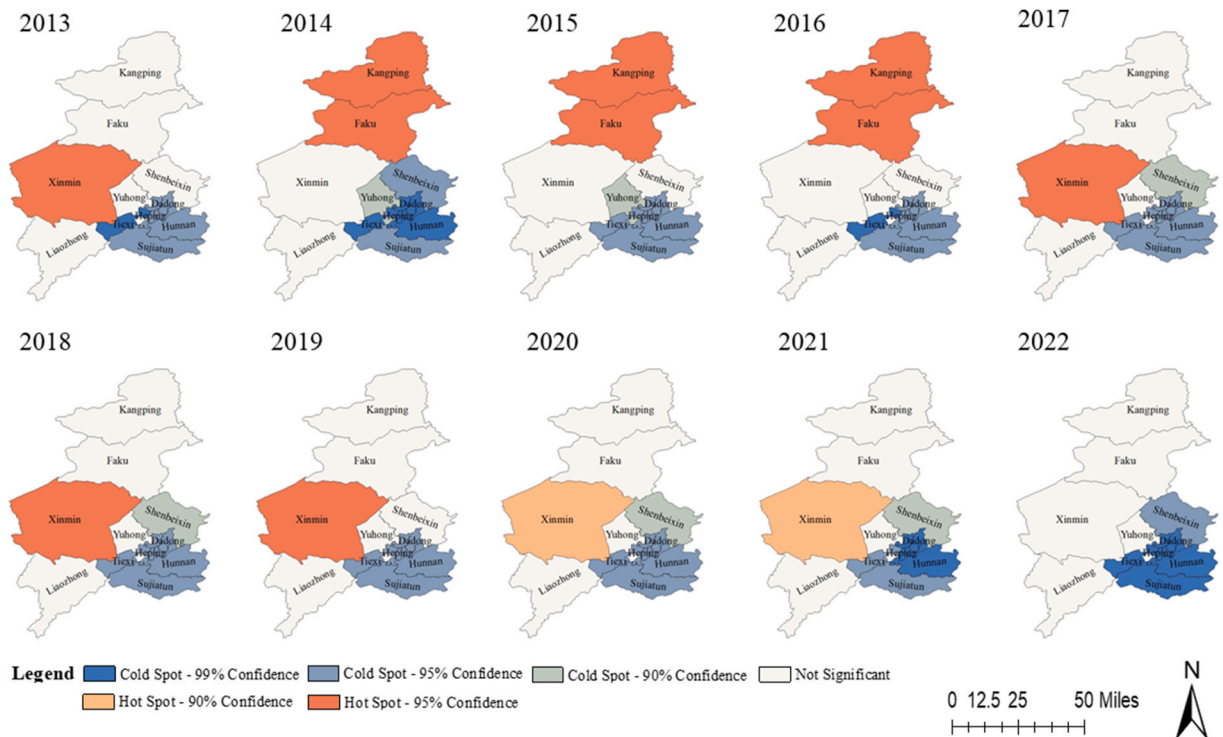


Fig. 4. Hotspot analysis (Getis-Ord, G_i^*) of the annual incidence of human brucellosis at districts/counties level in Shenyang, China, 2013–2022. Color depth indicates different Z-scores ranges. Districts with Z-scores >2.58 or Z-scores <-2.58 were considered to be significant at 99% confidence level ($P < 0.01$), and districts with Z-scores between 1.96 and 2.58 or Z-scores between $-2.58 \sim -1.96$ were considered to be significant at 95% confidence level ($P < 0.05$), and districts with Z-scores between 1.65 and 1.96 or Z-scores between $-1.96 \sim -1.65$ were considered to be significant at 90% confidence level ($P < 0.10$), and districts with Z-scores between $-1.65 \sim -1.65$ were considered to be no significant. These maps were produced by ArcGIS software version 10.8 (ESRI Inc., Redlands, California, USA). (For interpretation of the references to color in this figure legend, the reader is referred to the Web version of this article.)

prevent the emergence of new transmission routes.

Hotspot analysis helps in risk identification for early interventions to prevent outbreaks [52]. Our study indicated that the hotspot area exhibiting a significant high-high positive spatial association of HB incidence was situated around rural areas (Kangping, Faku, and Xinmin County), and the cold spot area exhibiting a significant low-low positive spatial association of HB incidence was observed in urban areas (Heping, Shenhe, Huanggu, Dadong, Tiexi District) and partial suburban areas (Handong, Sujiatun, Shenbeixin District), prompting us again that HB easily aggregated in rural areas. Interestingly, no hotspots were found in Shenyang during the three years of the COVID-19 epidemic from 2020 to 2022, even when the incidence of HB in rural areas, especially in Xinmin and Faku counties, increased significantly by 2021. In addition, the spatial relationship of HB in 2022 shows that all urban and suburban areas are cold spots, except for Yuhong District. This suggests that the spatial relationship of HB in Shenyang tended to be stable which aligns with our findings from the local spatial autocorrelation analysis, and that the outbreak risk of HB may be low.

In this study, the data from January 1, 2013 to December 31, 2022 were extracted from NIDRIS for the purpose of analysing the epidemic characteristics of reported HB in Shenyang, China. In our study, approximately 42% (3045/7187) of cases were excluded due to the patients residing outside of Shenyang. Further analysis revealed that the majority of the excluded cases came from surrounding cities in Liaoning province, such as Jinzhou (928 cases), Tieling (465 cases), Liaoyang (229 cases), Fuxin (200 cases), Anshan (179 cases), Chaoyang (171 cases), Huludao (160 cases), Yingkou (151 cases), Fushun (106 cases), Benxi (96 cases), Dandong (67 cases), Dalian (44 cases), and Panjin (33 cases). In addition, of the excluded cases, 98 were from the Inner Mongolia Autonomous Region, with 62 cases in Tongliao and 24 cases in Chifeng, all of which bordered Shenyang. This showed that Shenyang, especially the Sixth People’s Hospital of Shenyang (reported 2020 cases of excluded cases), played a significant part in the diagnosis and treatment of HB not only for local cases but also for imported cases from surrounding cities. Additionally, 39 duplicate cases were found, accounting for approximately 9.4/1000 (39/4142) of the total reported cases, indicating that the reporting mechanism of HB should further standardise management.

Finally, in this study, we visualized the spatial pattern of HB in Shenyang and identified high-risk regions, as well as proposed targeted directions for tackling HB in the future. However, despite the findings mentioned above, it is important to acknowledge the limitations of this study. Firstly, it should be noted that not all cases of HB were reported to the NIDRIS system. Therefore, while our analysis based on NIDRIS data provides insights into reported cases in Shenyang, it may not fully represent the actual incidence of HB in the local population. Secondly, our study revealed a higher likelihood of HB occurrence in rural areas and among farmers. This

observation suggests a potential link between the development of rural livestock husbandry and increased exposure to infected animals among farmers. To gain a deeper understanding of why there is a high incidence of HB among rural farmers, further investigation is warranted. For instance, a case-control study conducted in Shenyang aimed to explore possible factors contributing to this elevated risk among rural farmers.

5. Conclusions

Farmers in rural areas are the main population affected by HB, and more attention and resources should be allocated to protect this labour force. Rural areas were the hardest hit areas of HB, with notable worsening of incidence; therefore, it is crucial to enhance preventive and control measures for HB that specifically target rural areas. Suburban areas are where abnormally high values may occur, and measures for preventing the rebound of HB incidence in suburban areas should continue to be maintained. Although the annual incidence of HB in rural areas has increased, owing to the stability of spatial relationships and the disappearance of hotspots, there is little possibility of outbreaks; however, stricter monitoring should be applied in rural areas to prevent the emergence of new transmission routes. In addition, human's life is closely connected with livestock and their products, the concept of One Health should be fully recognized to tackle HB in the future.

Data availability statement

The datasets used and analysed in the current study are available from the corresponding author, Peng Li (E-mail: sylclp@163.com) upon reasonable request.

Ethics approval and consent to participate

The Ethics Committee of Shenyang Municipal Center for Disease Control and Prevention granted approval to the study protocol (No. 202301008) and all the enrolled subjects had written informed consent. For minors, this study not only obtained the consent of the minors themselves, but also obtained the consent of their parents/legal guardians, and wrote informed consent.

Consent for publication

Not applicable.

Funding

This study was not supported by any funding sources.

CRediT authorship contribution statement

Huijie Chen: Writing – review & editing, Writing – original draft, Methodology, Formal analysis, Data curation, Conceptualization. **Lihai Wen:** Formal analysis, Data curation. **Ye Chen:** Formal analysis, Data curation. **Xingyu Ji:** Formal analysis. **Peng Li:** Writing – review & editing, Supervision, Data curation, Conceptualization. **Wei Sun:** Supervision, Conceptualization.

Declaration of competing interest

The authors declare that they have no known competing financial interests or personal relationships that could have appeared to influence the work reported in this paper.

Acknowledgments

The authors wish to express their appreciation for the utilization of Microsoft Excel 2019, Joinpoint Regression Program(version 4.8.0.1), SPSS(version 23.0), and ArcGIS Desktop (version 10.8; Esri Lnc.; Redlands, California, USA) software tools in this study.

Abbreviations

HB	Human brucellosis
GIS	Geographic information system
APC	Annual percentage change
NIDRIS	Notifiable infectious disease reporting information system

Appendix A. Supplementary data

Supplementary data to this article can be found online at <https://doi.org/10.1016/j.heliyon.2024.e29026>.

References

- [1] M.J. Corbel, *Brucellosis in Humans and Animals*, World Health Organization, Geneva, 2006, p. 1.
- [2] Centers for Disease Control (CDC), *Brucellosis*. <https://www.cdc.gov/brucellosis>. (Accessed 30 May 2023).
- [3] K.A. Franc, R.C. Krecke, B.N. Hasler, et al., Brucellosis remains a neglected disease in the developing world: a call for interdisciplinary action, *BMC Publ. Health* 18 (1) (2018) 125, <https://doi.org/10.1186/s12889-017-5016-y>.
- [4] G. Pappas, N. Akritidis, M. Bosilkovski, et al., Brucellosis, *N. Engl. J. Med.* 352 (22) (2005) 2325–2336, <https://doi.org/10.1056/NEJMra050570>.
- [5] B.G. Mantur, S.K. Amarnath, R.S. Shinde, Review of clinical and laboratory features of human brucellosis, *Indian J. Med. Microbiol.* 25 (3) (2007) 188–202, <https://doi.org/10.4103/0255-0857.34758>.
- [6] M.P. Franco, M. Mulder, R.H. Gilman, et al., Human brucellosis, *Lancet Infect. Dis.* 7 (12) (2007) 775–786, [https://doi.org/10.1016/S1473-3099\(07\)70286-4](https://doi.org/10.1016/S1473-3099(07)70286-4).
- [7] J. Solera, Treatment of human brucellosis, *J. Med. Liban.* 48 (4) (2000) 255–263. <https://pubmed.ncbi.nlm.nih.gov/11214198/>.
- [8] R. Yousefi-Nooraie, S. Mortaz-Hejri, M. Mehrani, et al., Antibiotics for treating human brucellosis, *Cochrane Database Syst. Rev.* 10 (10) (2012) CD007179, <https://doi.org/10.1002/14651858.CD007179.pub2>.
- [9] M.N. Seleem, S.M. Boyle, N. Sriranganathan, Brucellosis: a re-emerging zoonosis, *Vet. Microbiol.* 140 (3–4) (2010) 392–398, <https://doi.org/10.1016/j.vetmic.2009.06.021>.
- [10] M. Bosilkovski, M. Dimzova, K. Grozdanovski, Natural history of brucellosis in an endemic region in different time periods, *Acta Clin. Croatica* 48 (1) (2009) 41–46. <https://pubmed.ncbi.nlm.nih.gov/19623871/>.
- [11] G.J. Jennings, R.A. Hajjeh, F.Y. Girgis, et al., Brucellosis as a cause of acute febrile illness in Egypt, *Trans. Roy. Soc. Trop. Med. Hyg.* 101 (7) (2007) 707–713, <https://doi.org/10.1016/j.trstmh.2007.02.027>.
- [12] G. Pappas, P. Papadimitriou, N. Akritidis, et al., The new global map of human brucellosis, *Lancet Infect. Dis.* 6 (2) (2006) 91–99, [https://doi.org/10.1016/S1473-3099\(06\)70382-6](https://doi.org/10.1016/S1473-3099(06)70382-6).
- [13] European Center for Disease Prevention and Control, *Brucellosis-annual epidemiological report for 2021*. <https://www.ecdc.europa.eu/en/publications-data/brucellosis-annual-epidemiological-report-2021>. (Accessed 31 May 2023).
- [14] World organization for animal health, *brucellosis*. <https://www.woah.org/en/disease/brucellosis>. (Accessed 31 May 2023).
- [15] I.I. Musallam, M.N. Abo-Shehadeh, Y.M. Hegazy, et al., Systematic review of brucellosis in the Middle East: disease frequency in ruminants and humans and risk factors for human infection, *Epidemiol. Infect.* 144 (4) (2016) 671–685. <https://doi.org/10.1017/S0950268815002575>.
- [16] S.J. Lai, H. Zhou, W.Y. Xiong, et al., Changing epidemiology of human brucellosis, China, 1955–2014, *Emerg. Infect. Dis.* 23 (2) (2017) 184–194, <https://doi.org/10.3201/eid2302.151710>.
- [17] P. Liang, Y. Zhao, J. Zhao, et al., The spatiotemporal distribution of human brucellosis in mainland China from 2007–2016, *BMC Infect. Dis.* 20 (1) (2020) 249, <https://doi.org/10.1186/s12879-020-4946-7>.
- [18] Z. Tao, Q. Chen, Y. Chen, et al., Epidemiological characteristics of human brucellosis-China, 2016–2019, *China CDC Wkly* 3 (6) (2021) 114–119, <https://doi.org/10.46234/ccdcw2021.030>.
- [19] L. Xu, Y. Deng, Spatiotemporal pattern evolution and driving factors of brucellosis in China, 2003–2019, *Int. J. Environ. Res. Publ. Health* 19 (16) (2022) 10082, <https://doi.org/10.3390/ijerph191610082>.
- [20] H. Yang, Q. Chen, Y. Li, et al., Epidemic characteristics, high-risk areas and space-time clusters of human brucellosis-China, 2020–2021, *China CDC Wkly* 5 (1) (2023) 17–22, <https://doi.org/10.46234/ccdcw2023.004>.
- [21] S. Lai, Q. Chen, Z. Li, Human brucellosis: an ongoing global health challenge, *China CDC Wkly* 3 (6) (2021) 120–123, <https://doi.org/10.46234/ccdcw2021.031>.
- [22] Ministry of Agriculture and Rural Affairs of China, *National brucellosis control program, 2016–2020* (in Chinese), http://www.moa.gov.cn/govpublic/SYJ/201609/t20160909_5270524.htm. (Accessed 10 January 2023).
- [23] Y.W. Sun, L.L. Mao, X. Li, et al., Epidemiological analysis of human brucellosis in Liaoning province from 2001 to 2011, *Chin. J. Vector Biol. Control* 23 (3) (2012) 268–269 (in Chinese).
- [24] Y.W. Sun, L.L. Mao, G.J. Sun, et al., Surveillance for brucellosis in Liaoning province, 2012–2015, *Disease Surveillance* 32 (3) (2017) 200–202, <https://doi.org/10.3784/j.issn.1003-9961.2017.03.008>, in Chinese).
- [25] W.J. Yu, Z.J. Wang, L.L. Mao, et al., Epidemiological characteristics of human brucellosis in Liaoning province, 2016–2020, *Disease Surveillance* 36 (12) (2021) 1257–1260, <https://doi.org/10.3784/jbjc.202110220326> (in Chinese).
- [26] P. Wang, X. Mao, Y. Gao, et al., Spatiotemporal distribution characteristic analysis of human brucellosis epidemic in Shenyang, China, 2009–2015, *Chin. J. Zoonoses* 35 (5) (2019) 455–459, <https://doi.org/10.3969/j.issn.1002-2694.2019.00.041> (in Chinese).
- [27] Shenyang Municipal Bureau of Statistics, *Shenyang statistical yearbook* (in Chinese), http://tj.shenyang.gov.cn/sjfb/nds/202211/t20221115_4332277.html. (Accessed 31 May 2023).
- [28] B. Arellano, J. Rocca, Defining urban and rural areas: a new approach, *Proc. SPIE* 10431, Remote Sensing Technologies and Applications in Urban Environments II 104310E (4 October 2017), <https://doi.org/10.1117/12.2277902>.
- [29] The National People's Congress of the People's Republic of China, *Law of the people's Republic of China on prevention and treatment of infectious diseases* (in Chinese), <http://www.npc.gov.cn/npc/c238/202001/099a493d03774811b058f0f0e38078.shtml>. (Accessed 31 May 2023).
- [30] Chinese Center for Disease Control and Prevention, *Reporting specifications for communicable diseases* (in Chinese), https://www.Chinacdc.cn/jkzt/crb/xcrxb/201810/t20181017_195160.html. (Accessed 31 May 2023).
- [31] National Health Commission of the People's Republic of China, *Diagnosis for brucellosis* (in Chinese), <http://www.nhc.gov.cn/wjw/s9491/201905/b109b71e7a624256985b573944b5d292/files/55d653517e924a01bb9aadceea7d93be.pdf>, 2019. (Accessed 31 May 2023).
- [32] M.M. Fischer, A. Getis, *Handbook of Applied Spatial Analysis*, Springer, Berlin Heidelberg, 2010, pp. 262–272, <https://doi.org/10.1007/978-3-642-03647-7>.
- [33] L. Anselin, Local indicators of spatial association-LISA, *Geogr. Anal.* 27 (1995) 93–115, <https://doi.org/10.1111/j.1538-4632.1995.tb00338.x>.
- [34] R. Pakzad, I. Pakzad, A. Janati, et al., Spatiotemporal analysis of brucellosis incidence in Iran from 2011–2014 using GIS, *Int. J. Infect. Dis.* 67 (2018) 129–136, <https://doi.org/10.1016/j.ijid.2017.10.017>.
- [35] C. Zhao, K. Liu, C. Jiang, et al., Epidemic characteristics and transmission risk prediction of brucellosis in Xi'an city, Northwest China, *Front. Public Health* 10 (2022) 926812, <https://doi.org/10.3389/fpubh.2022.926812>.
- [36] Q. Chen, S. Lai, W. Yin, et al., Epidemic characteristics, high-risk townships and space-time clusters of human brucellosis in Shanxi Province of China, 2005–2014, *BMC Infect. Dis.* 16 (1) (2016) 760, <https://doi.org/10.1186/s12879-016-2086-x>.
- [37] T. Wang, X. Wang, P. Tie, et al., Spatio-temporal cluster and distribution of human brucellosis in Shanxi Province of China between 2011 and 2016, *Sci. Rep.* 8 (1) (2018) 16977, <https://doi.org/10.1038/s41598-018-34975-7>, 2018.
- [38] D. Liang, D. Liu, M. Yang, et al., Spatiotemporal distribution of human brucellosis in Inner Mongolia, China, in 2010–2015, and influencing factors, *Sci. Rep.* 11 (1) (2021) 24213, <https://doi.org/10.1038/s41598-021-03723-9>.
- [39] D. Li, L. Li, J. Zhai, et al., Epidemiological features of human brucellosis in Tongliao City, Inner Mongolia province, China: a cross-sectional study over an 11-year period (2007–2017), *BMJ Open* 10 (1) (2020) e031206, <https://doi.org/10.1136/bmjopen-2019-031206>.
- [40] X.L. Yu, Q. Li, Y.X. Pei, et al., Analysis on the epidemiological characteristics of brucellosis related public health emergencies in Shandong Province from 2012 to 2022, *J. Trop. Dis. Parasitol.* 21 (3) (2023) 146–149, <https://doi.org/10.3969/j.issn.1672-2302.2023.03.006> (in Chinese).
- [41] X.L. Wu, R.T. Qi, F. Yan, et al., Analysis of epidemiological characteristics and prediction of incidence trend of brucellosis in Ningxia from 2012 to 2021, *Ningxia Med. J.* 45 (2) (2023) 107–109, <https://doi.org/10.13621/j.1001-5949.2023.02.0107> (in Chinese).
- [42] W.Y. Zhang, L.L. Zhao, Epidemiological characteristics of human brucellosis in Hebi city, Henan province, 2008–2022, *Modern Disease Control and Prevention* 34 (9) (2023) 675–678, <https://doi.org/10.13515/j.cnki.hnjpm.1006-8414.2023.09.008> (in Chinese).

- [43] J.X. Ge, S.H. Yin, L. Tang, et al., Epidemiological characteristics of human brucellosis in heilongjiang province, 2012-2022, chin. J. Public Health Eng. 22 (6) (2023) 729–731, <https://doi.org/10.19937/j.issn.1671-4199.2023.06.003> (in Chinese).
- [44] Z.G. Liu, M. Wang, N. Ta, et al., Seroprevalence of human brucellosis and molecular characteristics of Brucella strains in Inner Mongolia Autonomous region of China, from 2012 to 2016, Emerg. Microb. Infect. 9 (1) (2020) 263–274, <https://doi.org/10.1080/22221751.2020.1720528>.
- [45] X.P. Cheng, Y.B. Zhou, X.W. Li, et al., Analysis of influencing factors about brucellosis among occupational groups in western Liaoning province, J. Environ. Occup. Med. 27 (5) (2010) 314–316, <https://doi.org/10.13213/j.cnki.jeom.2010.05.021> (in Chinese).
- [46] R.L. Lu, H.R. Sun, Y.H. Zhu, et al., Awareness of brucellosis prevention knowledge and risk behavior prevalence among people in high-risk population in Ruzhou, Henan, Disease Surveillance 28 (7) (2013) 564–567, <https://doi.org/10.3784/j.issn.1003-9961.2013.7.014> (in Chinese).
- [47] Z. Yang, M. Pang, Q. Zhou, et al., Spatiotemporal expansion of human brucellosis in Shaanxi Province, Northwestern China and model for risk prediction, PeerJ 8 (2020) e10113, <https://doi.org/10.7717/peerj.10113>.
- [48] H.T. Yuan, C.L. Wang, W.N. Liu, et al., Epidemiologically characteristics of human brucellosis and antimicrobial susceptibility pattern of Brucella melitensis in Hinggan League of the Inner Mongolia Autonomous Region, China, Infect. Dis. Poverty 9 (1) (2020) 79, <https://doi.org/10.1186/s40249-020-00697-0>.
- [49] J. Huang, G.R. Mclean, F.C. Dubee, et al., Two pandemics in China, one health in Chinese, BMJ Glob. Health 7 (3) (2022) e008550, <https://doi.org/10.1136/bmjgh-2022-008550>.
- [50] Y.J. Li, X.L. Li, S. Liang, et al., Epidemiological features and risk factors associated with the spatial and temporal distribution of human brucellosis in China, BMC Infect. Dis. 13 (2013) 547, <https://doi.org/10.1186/1471-2334-13-547>.
- [51] P.F. Liang, Y. Zhao, J.H. Zhao, et al., Human distribution and spatial-temporal clustering analysis of human brucellosis in China from 2012 to 2016, Infect. Dis. Poverty 9 (1) (2020) 142, <https://doi.org/10.1186/s40249-020-00754-8>.
- [52] S. Chakravorty, Identifying crime clusters: the spatial principles, Middle States Geographer 28 (1995) 53–58.